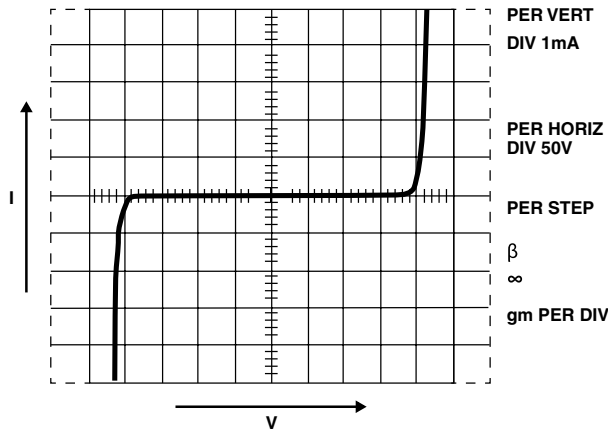


**What Is A Littelfuse Varistor?**

Varistors are voltage dependent, nonlinear devices which have an electrical behavior similar to back-to-back zener diodes. The symmetrical, sharp breakdown characteristics shown in Figure 1 enable the varistor to provide excellent transient suppression performance. When exposed to high voltage transients the varistor impedance changes many orders of magnitude from a near open circuit to a highly conductive level, thus clamping the transient voltage to a safe level. The potentially destructive energy of the incoming transient pulse is absorbed by the varistor, thereby protecting vulnerable circuit components.



**FIGURE 1. TYPICAL VARISTOR V-I CHARACTERISTIC**

The varistor is composed primarily of zinc oxide with small additions of bismuth, cobalt, manganese and other metal oxides. The structure of the body consists of a matrix of conductive zinc oxide grains separated by grain boundaries providing P-N junction semiconductor characteristics. These boundaries are responsible for blocking conduction at low voltages and are the source of the nonlinear electrical conduction at higher voltages.

Since electrical conduction occurs, in effect, between zinc oxide grains distributed throughout the bulk of the device, the Littelfuse Varistor is inherently more rugged than its single P-N junction counterparts, such as zener diodes. In the varistor, energy is absorbed uniformly throughout the body of the device with the resultant heating spread evenly through its volume. Electrical properties are controlled mainly by the physical dimensions of the varistor body which is sintered in various form factors such as discs, chips and tubes. The energy rating is determined by volume, voltage rating by thickness or current flow path length, and current capability by area measured normal to the direction of current flow.

Littelfuse Varistors are available with AC operating voltages from 2.5V to 6000V. Higher voltages are limited only by packaging ability. Peak current handling exceeds 70,000A and energy capability extends beyond 10,000J for the larger units. Package styles include the tiny multilayer surface mount suppressors, tubular devices for use in connectors, and progress in size up to the rugged industrial device line.

**Physical Properties**

**Introduction**

An attractive property of the metal oxide varistor, fabricated from zinc oxide (ZnO), is that the electrical characteristics are related to the bulk of the device. Each ZnO grain of the ceramic acts as if it has a semiconductor junction at the grain boundary. A cross-section of the material is shown in Figure 2, which illustrates the ceramic microstructure. The ZnO grain boundaries can be clearly observed. Since the nonlinear electrical behavior occurs at the boundary of each semiconducting ZnO grain, the varistor can be considered a "multi-junction" device composed of many series and parallel connections of grain boundaries. Device behavior may be analyzed with respect to the details of the ceramic microstructure. Mean grain size and grain size distribution play a major role in electrical behavior.

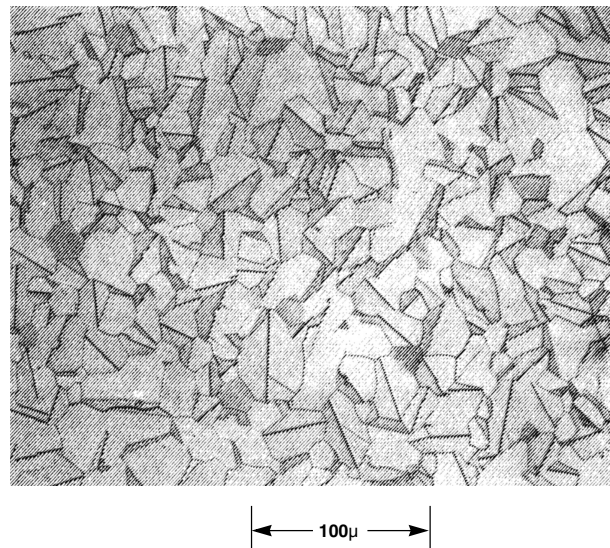


**FIGURE 2. OPTICAL PHOTOMICROGRAPH OF A POLISHED AND ETCHED SECTION OF A VARISTOR**

**Varistor Microstructure**

Varistors are fabricated by forming and sintering zinc oxide-based powders into ceramic parts. These parts are then electroded with either thick film silver or arc/flame sprayed metal. The bulk of the varistor between contacts is comprised of ZnO grains of an average size “d” as shown in the schematic model of Figure 3. Resistivity of the ZnO is <math><0.3\Omega\text{-cm}</math>.

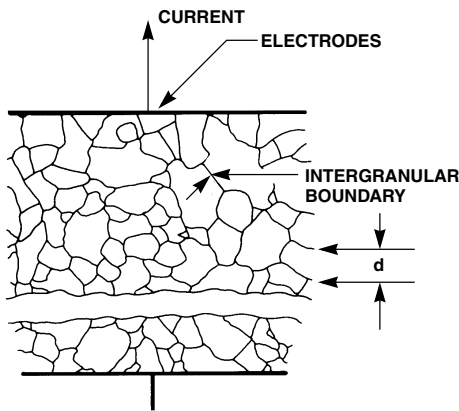


**FIGURE 3. SCHEMATIC DEPICTION OF THE MICROSTRUCTURE OF A METAL-OXIDE VARISTOR. GRAINS OF CONDUCTING ZnO (AVERAGE SIZE d) ARE SEPARATED BY INTERGRANULAR BOUNDARIES**

Designing a varistor for a given nominal varistor voltage,  $V_N$ , is basically a matter of selecting the device thickness such that the appropriate number of grains,  $n$ , are in series between electrodes. In practice, the varistor material is characterized by a voltage gradient measured across its thickness by a specific volts/mm value. By controlling composition and manufacturing conditions the gradient remains fixed. Because there are practical limits to the range of thicknesses achievable, more than one voltage gradient value is desired. By altering the composition of the metal oxide additives it is possible to change the grain size “d” and achieve the desired result.

A fundamental property of the ZnO varistor is that the voltage drop across a single interface “junction” between grains is nearly constant. Observations over a range of compositional variations and processing conditions show a fixed voltage drop of about 2V-3V per grain boundary junction. Also, the voltage drop does not vary for grains of different sizes.

It follows, then, that the varistor voltage will be determined by the thickness of the material and the size of the ZnO grains. The relationship can be stated very simply as follows:

$$\text{Varistor Voltage, } V_N(\text{DC}) = (3V)n$$

Where,  $n$  = average number of grain boundaries between electrodes

$$\text{and, varistor thickness, } D = (n + 1)d \approx \frac{V_N \times d}{3}$$

where,  $d$  = average grain size

The varistor voltage,  $V_N$ , is defined as the voltage across a varistor at the point on its V-I characteristic where the transition is complete from the low-level linear region to the highly nonlinear region. For standard measurement purposes, it is arbitrarily defined as the voltage at a current of 1mA.

Some typical values of dimensions for Littelfuse Varistors are given in Table 1.

**TABLE 1.**

VARISTOR VOLTAGE	AVERAGE GRAIN SIZE	n	GRADIENT	DEVICE THICKNESS
VOLTS	MICRONS		V/mm AT 1mA	mm
150V <sub>RMS</sub>	20	75	150	1.5
25V <sub>RMS</sub>	80 (Note)	12	39	1.0

NOTE: Low voltage formulation.

**Theory of Operation**

Because of the polycrystalline nature of metal-oxide semiconductor varistors, the physical operation of the device is more complex than that of conventional semiconductors. Intensive measurement has determined many of the device's electrical characteristics, and much effort continues to better define the varistor's operation. In this application note we will discuss some theories of operation, but from the user's viewpoint this is not nearly as important as understanding the basic electrical properties as they relate to device construction.

The key to explaining metal-oxide varistor operation lies in understanding the electronic phenomena occurring near the grain boundaries, or junctions between the zinc oxide grains. While some of the early theory supposed that electronic tunneling occurred through an insulating second phase layer at the grain boundaries, varistor operation is probably better described by a series-parallel arrangement of semiconducting diodes. In this model, the grain boundaries contain defect states which trap free electrons from the n-type semiconducting zinc oxide grains, thus forming a space charge depletion layer in the ZnO grains in the region adjacent to the grain boundaries [6].

Evidence for depletion layers in the varistor is shown in Figure 4 where the inverse of the capacitance per boundary squared is plotted against the applied voltage per boundary [7]. This is the same type of behavior observed

for semiconductor abrupt P-N junction diodes. The relationship is:

$$\frac{1}{C^2} = \frac{2(V_b + V)}{q\epsilon s N}$$

Where  $V_b$  is the barrier voltage,  $V$  the applied voltage,  $q$  the electron charge,  $\epsilon s$  the semiconductor permittivity and  $N$  is the carrier concentration. From this relationship the ZnO carrier concentration,  $N$ , was determined to be about  $2 \times 10^{17}$  per  $\text{cm}^3$  [7]. In addition, the width of the depletion layer was calculated to be about 1000 Angstrom units. Single junction studies also support the diode model [9].

It is these depletion layers that block the free flow of carriers and are responsible for the low voltage insulating behavior in the leakage region as depicted in Figure 5. The leakage current is due to the free flow of carriers across the field lowered barrier, and is thermally activated, at least above about  $25^\circ\text{C}$ .

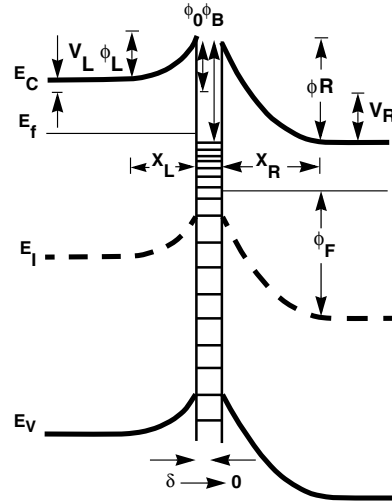


FIGURE 5. ENERGY BAND DIAGRAM OF A ZnO-GRAINBOUNDARY-ZnO JUNCTION

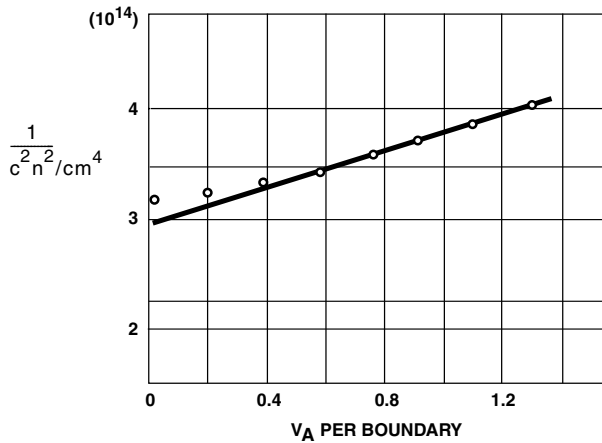


FIGURE 4. CAPACITANCE-VOLTAGE BEHAVIOR OF VARISTOR RESEMBLES A SEMICONDUCTOR ABRUPT-JUNCTION REVERSED BIASED DIODE  $N_d \sim 2 \times 10^{17}/\text{cm}^3$

Figure 5 shows an energy band diagram for a ZnO-grain boundary-ZnO junction [10]. The left-hand grain is forward biased,  $V_L$ , and the right side is reverse biased to  $V_R$ . The depletion layer widths are  $X_L$  and  $X_R$ , and the respective barrier heights are  $\phi_L$  and  $\phi_R$ . The zero biased barrier height is  $\phi_0$ . As the voltage bias is increased,  $\phi_L$  is decreased and  $\phi_R$  is increased, leading to a lowering of the barrier and an increase in conduction.

The barrier height  $\phi_L$  of a low voltage varistor was measured as a function of applied voltage [11], and is presented in Figure 6. The rapid decrease in the barrier at high voltage represents the onset of nonlinear conduction [12].

Transport mechanisms in the nonlinear region are very complicated and are still the subject of active research. Most theories draw their inspiration from semiconductor transport theory and the reader is referred to the literature for more information [3, 5, 13, 14, 15].

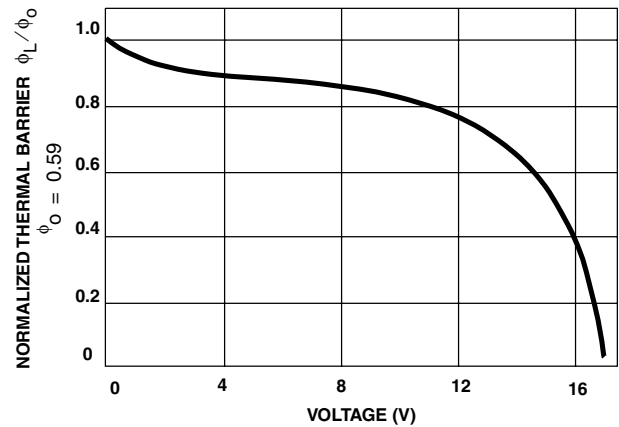


FIGURE 6. THERMAL BARRIER vs APPLIED VOLTAGE

Turning now to the high current upturn region in Figure 10, we see that the V-I behavior approaches an ohmic characteristic. The limiting resistance value depends upon the electrical conductivity of the body of the semiconducting ZnO grains, which have carrier concentrations in the range of  $10^{17}$  to  $10^{18}$  per  $\text{cm}^3$ . This would put the ZnO resistivity below  $0.3\Omega\text{cm}$ .

### Varistor Construction

The process of fabricating a Littelfuse Varistor is illustrated in the flow chart of Figure 7. The starting material may differ in the composition of the additive oxides, in order to cover the voltage range of product.

## Application Note 9767

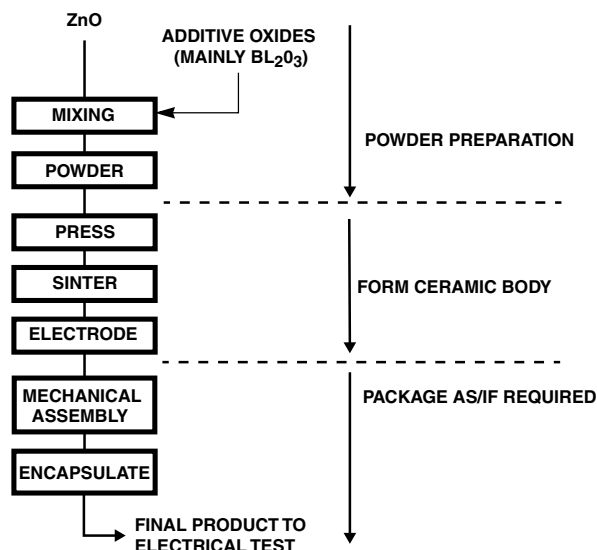


**FIGURE 7. SCHEMATIC FLOW DIAGRAM OF LITTELFUSE VARISTOR FABRICATION**

Device characteristics are determined at the pressing operation. The powder is pressed into a form of predetermined thickness in order to obtain a desired value of nominal voltage. To obtain the desired ratings of peak current and energy capability, the electrode area and mass of the device are varied. The range of diameters obtainable in disc product offerings is listed here:

Nominal Disc Diameter - mm	3	5	7	10	14	20	32	34	40	62
----------------------------	---	---	---	----	----	----	----	----	----	----

Of course, other shapes, such as rectangles, are also possible by simply changing the press dies. Other ceramic fabrication techniques can be used to make different shapes. For example, rods or tubes are made by extruding and cutting to length. After forming, the green (i.e., unfired) parts are placed in a kiln and sintered at peak temperatures in excess of 1200°C. The bismuth oxide is molten above 825°C, assisting in the initial densification of the polycrystalline ceramic. At higher temperatures, grain growth occurs, forming a structure with controlled grain size.

Electroding is accomplished, for radial and chip devices, by means of thick film silver fired onto the ceramic surface. Wire leads or strap terminals are then soldered in place. A conductive epoxy is used for connecting leads to the axial 3mm discs. For the larger industrial devices (40mm and 60mm diameter discs) the contact material is arc sprayed aluminum, with an overspray of copper if necessary to give a solderable surface.

Many encapsulation techniques are used in the assembly of the various Littelfuse Varistor packages. Most radials and some industrial devices (HA Series) are epoxy coated in a fluidized bed, whereas epoxy is “spun” onto the axial device.

Radials are also available with phenolic coatings applied using a wet process. The PA series package consists of plastic molded around a 20mm disc subassembly. The RA, DA, and DB series devices are all similar in that they all are composed of discs or chips, with tabs or leads, encased in a molded plastic shell filled with epoxy. Different package styles allow variation in energy ratings, as well as in mechanical mounting. Figures 8 and 9 illustrate several package forms.

Figure 9 shows construction details of some packages. Dimensions of the ceramic, by package type, are given in Table 2.

**TABLE 2. BY-TYPE CERAMIC DIMENSIONS**

PACKAGE TYPE	SERIES	CERAMIC DIMENSIONS
Leadless Surface Mount	CH, AUML†, ML†, MLE†, MLN† Series	5mm x 8mm Chip, 0603, 0805, 1206, 1210, 1812, 2220
Connector Pin	CP Series	22, 20, 16 ID Gauge Tube
Axial Leaded	MA Series	3mm Diameter Disc
Radial Leaded	ZA, LA, “C” III, UltraMOV™ Series	5mm, 7mm, 10mm, 14mm, 20mm Diameter Discs
Boxed, Low Profile	RA Series	5mm x 8mm, 10mm x 16mm, 14 x 22 Chips
Industrial Packages	PA Series HA Series HB Series DA, DB Series BA, BB Series	20mm Diameter Disc 32mm, 40mm Diameter Disc 34mm Square Disc 40mm Diameter Disc 60mm Diameter Disc
Industrial Discs	CA, NA Series	32mm, 40mm, 60mm Diameter Discs, 34mm Square
Arrester	AS Series	32mm, 42mm, 60mm Diameter Discs

† Littelfuse multilayer suppressor technology devices.

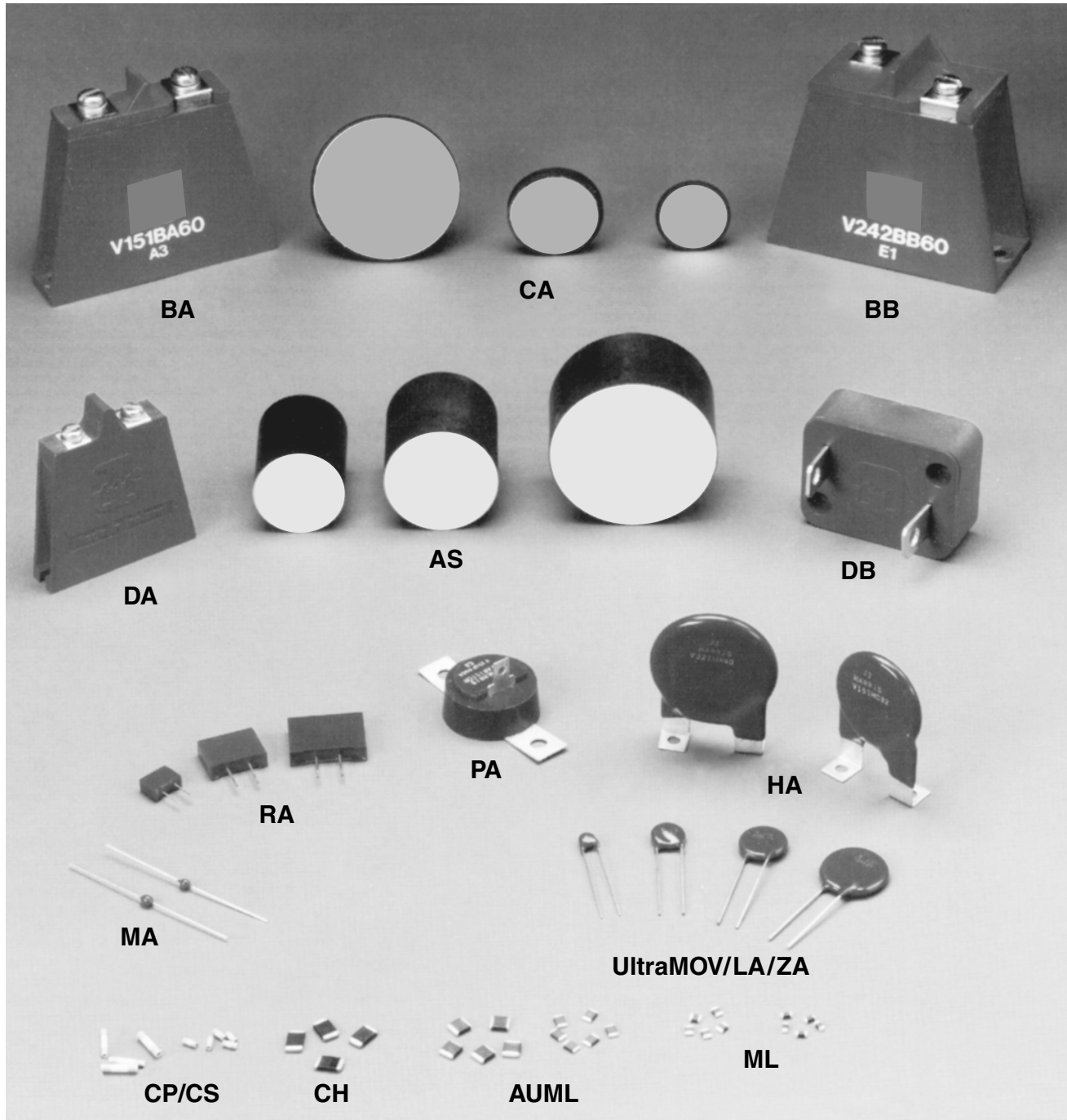


FIGURE 8. PACKAGE FORMS



FIGURE 9A. CROSS-SECTION OF MA PACKAGE

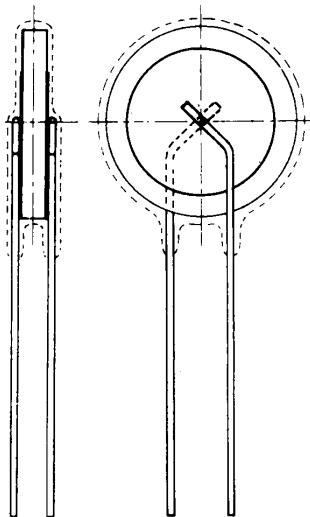


FIGURE 9B. CROSS-SECTION OF RADIAL LEAD PACKAGE

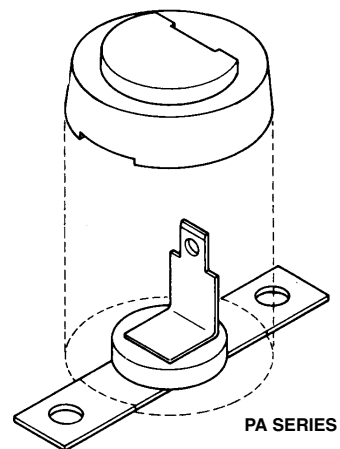
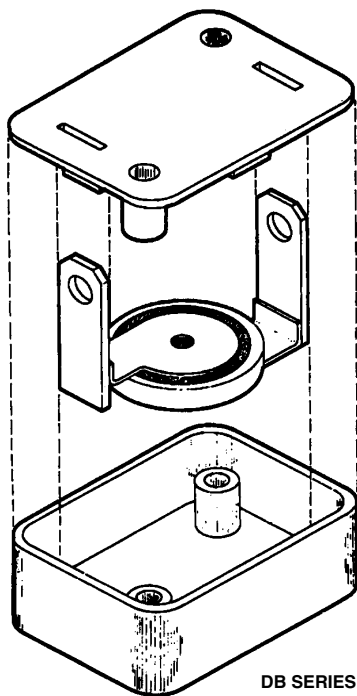
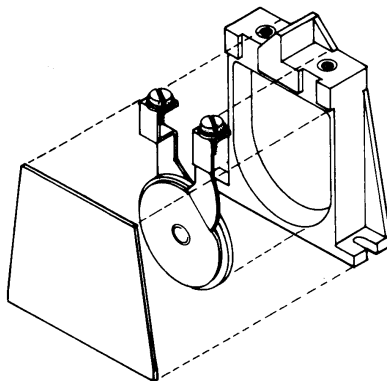


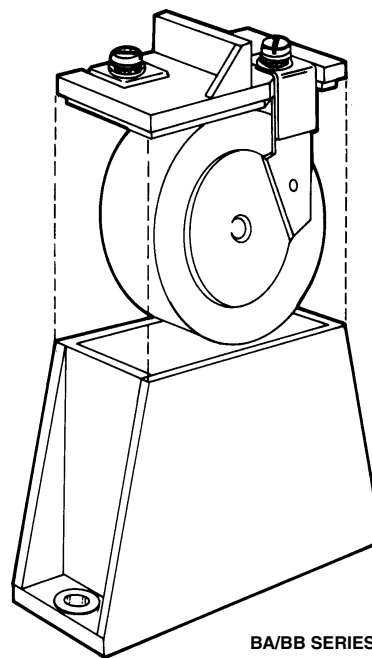
FIGURE 9C. PICTORIAL VIEW OF POWER MOV PACKAGE



DB SERIES



DA SERIES



BA/BB SERIES

FIGURE 9D. PICTORIAL VIEW OF HIGH ENERGY PACKAGES, DA, DB, AND BA/BB SERIES

## Electrical Characterization

### Varistor VI Characteristics

Varistor electrical characteristics are conveniently displayed using log-log format in order to show the wide range of the V-I curve. The log format also is clearer than a linear representation which tends to exaggerate the nonlinearity in proportion to the current scale chosen. A typical V-I

characteristic curve is shown in Figure 10. This plot shows a wider range of current than is normally provided on varistor data sheets in order to illustrate three distinct regions of electrical operation.

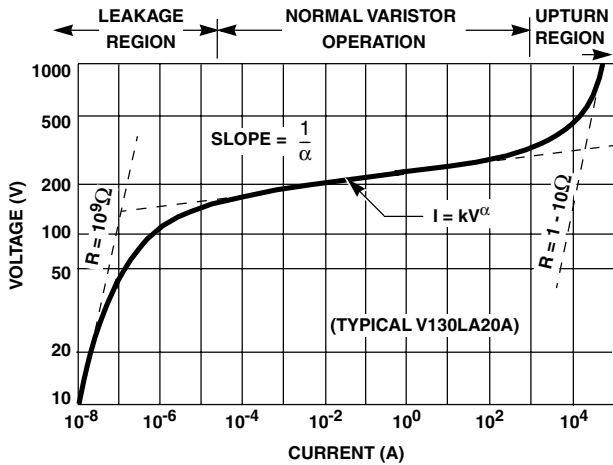


FIGURE 10. TYPICAL VARISTOR V-I CURVE PLOTTED ON LOG-LOG SCALE

**Equivalent Circuit Model**

An electrical model for the varistor can be represented by the simplified equivalent circuit of Figure 11.

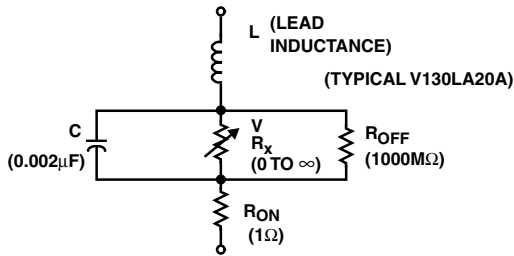


FIGURE 11. VARISTOR EQUIVALENT CIRCUIT MODEL

**Leakage Region of Operation**

At low current levels, the V-I Curve approaches a linear (ohmic) relationship and shows a significant temperature dependence. The varistor is in a high resistance mode (approaching  $10^9 \Omega$ ) and appears as an open circuit. The nonlinear resistance component,  $R_X$ , can be ignored because  $R_{OFF}$  in parallel will predominate. Also,  $R_{ON}$  will be insignificant compared to  $R_{OFF}$ .

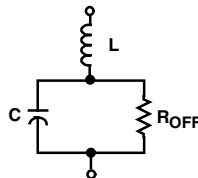


FIGURE 12. EQUIVALENT CIRCUIT AT LOW CURRENTS

For a given varistor device, capacitance remains approximately constant over a wide range of voltage and frequency in the leakage region. The value of capacitance drops only slightly as voltage is applied to the varistor. As the voltage approaches the nominal varistor voltage, the

capacitance abruptly decreases. Capacitance remains nearly constant with frequency change up to 100kHz. Similarly, the change with temperature is small, the 25°C value of capacitance being well within  $\pm 10\%$  from -40°C to 125°C.

The temperature effect of the V-I characteristic curve in the leakage region is shown in Figure 13. A distinct temperature dependence is noted.

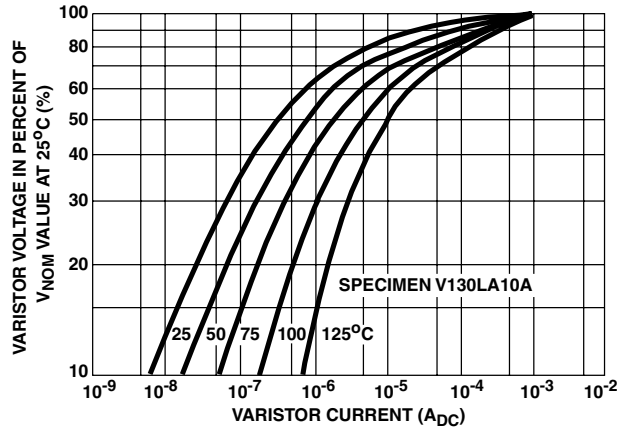


FIGURE 13. TEMPERATURE DEPENDENCE OF THE CHARACTERISTIC CURVE IN THE LEAKAGE REGION

The relation between the leakage current,  $I$ , and temperature,  $T$ , is:

$$I = I_0 \epsilon^{-V_B/kT}$$

where:  $I_0$  = constant  
 $k$  = Boltzmann's Constant  
 $V_B = 0.9eV$

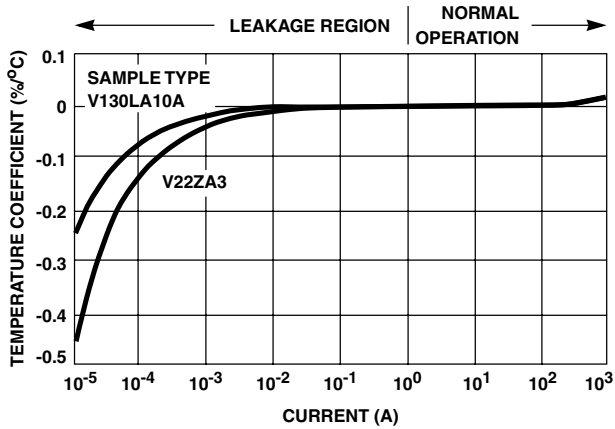
The temperature variation, in effect, corresponds to a change in  $R_{OFF}$ . However,  $R_{OFF}$  remains at a high resistance value even at elevated temperatures. For example, it is still in the range of 10M $\Omega$  to 100M $\Omega$  at 125°C.

Although  $R_{OFF}$  is a high resistance it varies with frequency. The relationship is approximately linear with inverse frequency.

$$R_{OFF} \sim \frac{1}{f}$$

However, the parallel combination of  $R_{OFF}$  and  $C$  is predominantly capacitive at any frequency of interest. This is because the capacitive reactance also varies approximately linearly with  $1/f$ .

At higher currents, at and above the milliamp range, temperature variation becomes minimal. The plot of the temperature coefficient ( $DV/DT$ ) is given in Figure 14. It should be noted that the temperature coefficient is negative and decreases as current rises. In the clamping voltage range of the varistor ( $I > 1A$ ), the temperature dependency approaches zero.



NOTE: Typical Temperature Coefficient of Voltage vs Current, 14mm Size, 55°C to 125°C.

FIGURE 14. RELATION OF TEMPERATURE COEFFICIENT DV/DT TO VARISTOR CURRENT

**Normal Varistor Region of Operation**

The varistor characteristic follows the equation  $I = kV^\alpha$ , where k is a constant and the exponent  $\alpha$  defines the degree of nonlinearity. Alpha is a figure of merit and can be determined from the slope of the V-I curve or calculated from the formula:

$$\alpha = \frac{\log(I_2/I_1)}{\log(V_2/V_1)}$$

$$= \frac{1}{\log(V_2/V_1)} \text{ for } I_2/I_1 = 1$$

In this region the varistor is conducting and  $R_X$  will predominate over C,  $R_{ON}$  and  $R_{OFF}$ .  $R_X$  becomes many orders of magnitude less than  $R_{OFF}$  but remains larger than  $R_{ON}$ .

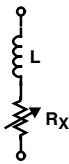


FIGURE 15. EQUIVALENT CIRCUIT AT VARISTOR CONDUCTION

During conduction the varistor voltage remains relatively constant for a change in current of several orders of magnitude. In effect, the device resistance,  $R_X$ , is changing in response to current. This can be observed by examining the static or dynamic resistance as a function of current. The static resistance is defined by:

$$R_X = \frac{V}{I}$$

and the dynamic resistance by:

$$Z_X = \frac{dv}{di} = V/\alpha I = R_X/\alpha$$

Plots of typical resistance values vs current, I, are given in Figure 16.

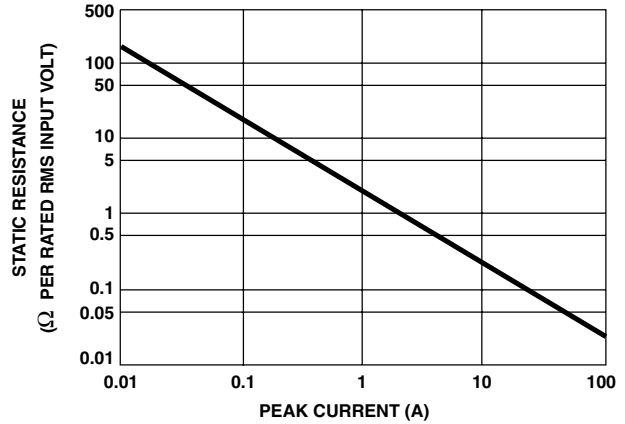


FIGURE 16A.  $R_X$  STATIC VARISTOR RESISTANCE FIGURE

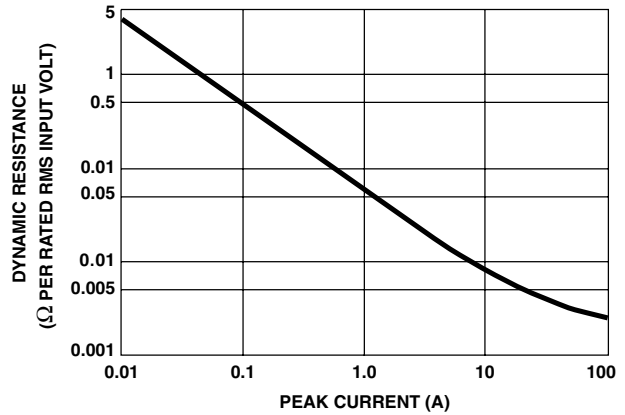


FIGURE 16B.  $Z_X$  DYNAMIC VARISTOR RESISTANCE

**Upturn Region of Operation**

At high currents, approaching the maximum rating, the varistor approximates a short-circuit. The curve departs from the nonlinear relation and approaches the value of the material bulk resistance, about 1Ω-10Ω. The upturn takes place as  $R_X$  approaches the value of  $R_{ON}$ . Resistor  $R_{ON}$  represents the bulk resistance of the zinc oxide grains. This resistance is linear (which appears as a steeper slope on the log plot) and occurs at currents 50A to 50,000A, depending on the varistor size.

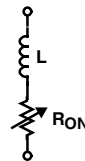
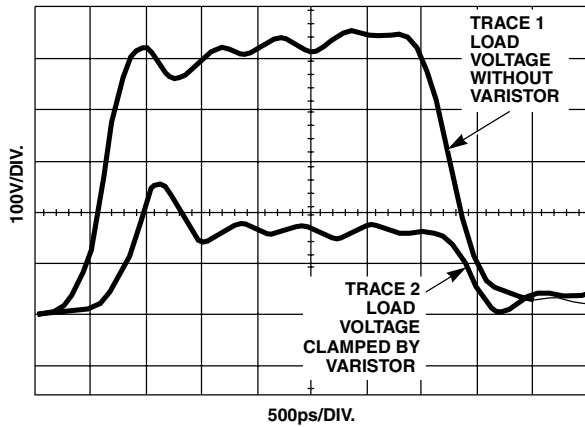


FIGURE 17. EQUIVALENT CIRCUIT AT VARISTOR UPTURN



**Speed of Response and Rate Effects**

The varistor action depends on a conduction mechanism similar to that of other semiconductor devices. For this reason, conduction occurs very rapidly, with no apparent time lag - even into the nanosecond range. Figure 18 shows a composite photograph of two voltage traces with and without a varistor inserted in a very low inductance impulse generator. The second trace (which is not synchronized with the first, but merely superimposed on the oscilloscope screen) shows that the voltage clamping effect of the varistor occurs in less than one nanosecond.



**FIGURE 18. RESPONSE OF A ZnO VARISTOR TO A FAST RISE TIME (500ps) PULSE**

In the conventional lead-mounted devices, the inductance of the leads would completely mask the fast action of the varistor; therefore, the test circuit for Figure 18 required insertion of a small piece of varistor material in a coaxial line to demonstrate the intrinsic varistor response.

Tests made on lead mounted devices, even with careful attention to minimizing lead length, show that the voltages induced in the loop formed by the leads contribute a substantial part of the voltage appearing across the terminals of a varistor at high current and fast current rise. Fortunately, the currents which can be delivered by a transient source are invariably slower in rise time than the observed voltage transients. The applications most frequently encountered for varistors involve current rise times longer than 0.5μs.

Voltage rate-of-rise is not the best term to use when discussing the response of a varistor to a fast impulse (unlike spark gaps where a finite time is involved in switching from nonconducting to conducting state). The response time of the varistor to the transient current that a circuit can deliver is the appropriate characteristic to consider.

The V-I characteristic of Figure 19A shows how the response of the varistor is affected by the current waveform. From such data, an "overshoot" effect can be defined as being the relative increase in the maximum voltage appearing across the varistor during a fast current rise, using the conventional 8/20μs current wave as the reference. Figure 19B shows typical clamping voltage variation with rise time for various current levels.

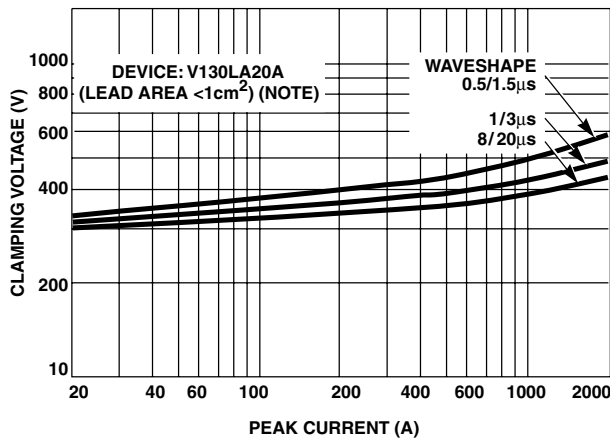


**FIGURE 19A. V-I CHARACTERISTICS FOR VARIOUS CURRENT RISE TIMES**

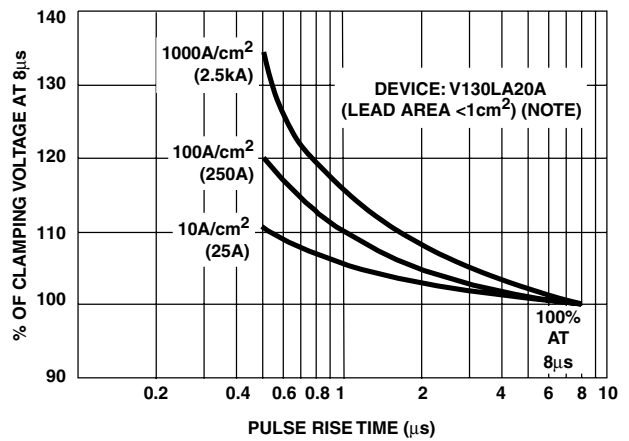


**FIGURE 19B. OVERSHOOT DEFINED WITH REFERENCE TO THE BASIC 8/20μs CURRENT PULSE**

NOTE: Refer to the Maximum Clamping Voltage section of DB450, Transient Voltage Suppression Devices.

**FIGURE 19. RESPONSE OF LEAD-MOUNTED VARISTORS TO CURRENT WAVEFORM**

**Varistor Terminology**

The following tabulation defines the terminology used in varistor specifications. Existing standards have been followed wherever possible.

**Definitions (IEEE Standard C62.33, 1982)**

A characteristic is an inherent and measurable property of a device. Such a property may be electrical, mechanical, or thermal, and can be expressed as a value for stated conditions.

A rating is a value which establishes either a limiting capability or a limiting condition (either maximum or minimum) for operation of a device. It is determined for specified values of environment and operation. The ratings indicate a level of stress which may be applied to the device without causing degradation or failure. Varistor symbols are defined on the linear V-I graph illustrated in Figure 20.

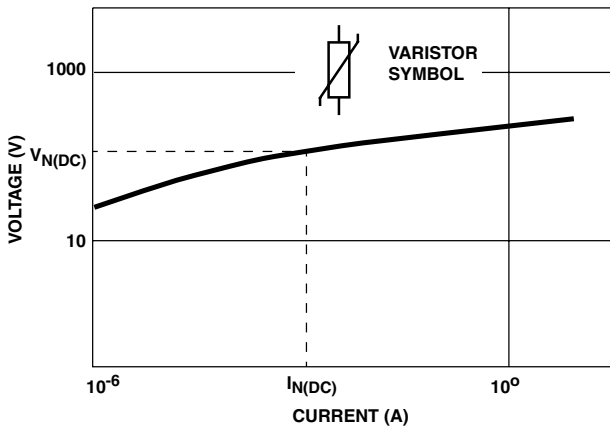
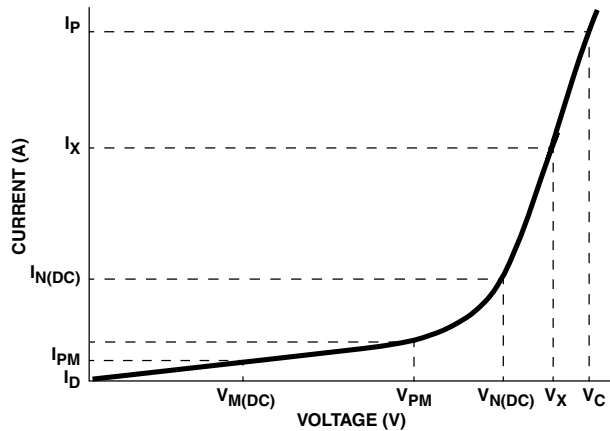


FIGURE 20. I-V GRAPH ILLUSTRATING SYMBOLS AND DEFINITIONS

**Test Waveform**

At high current and energy levels, varistor characteristics are measured, of necessity, with an impulse waveform. Shown in Figure 21 is the ANSI Standard C62.1 waveshape, an exponentially decaying waveform representative of lightning surges and the discharge of stored energy in reactive circuits.

The 8/20μs current wave (8μs rise and 20μs to 50% decay of peak value) is used as a standard, based on industry practices, for the characteristics and ratings described. One exception is the energy rating ( $W_{TM}$ ), where a longer waveform of 10/1000μs is used. This condition is more representative of the high energy surges usually experienced from inductive discharge of motors and transformers. Varistors are rated for a maximum pulse energy surge that results in a varistor voltage ( $V_N$ ) shift of less than ±10% from initial value.

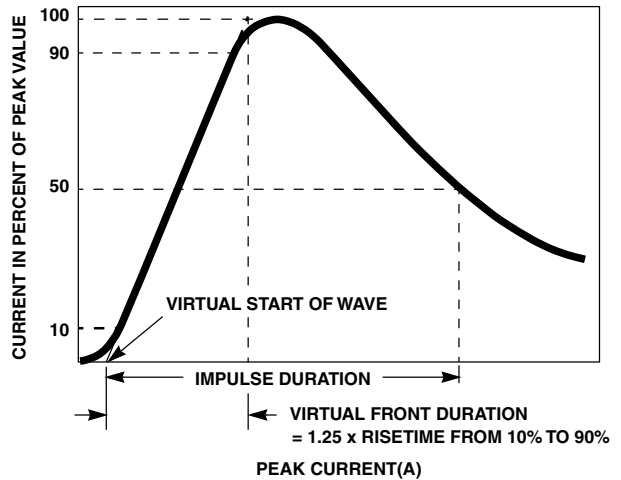


FIGURE 21. DEFINITION OF PULSE CURRENT WAVEFORM

## Application Note 9767

**TABLE 3. VARISTOR CHARACTERISTICS (IEEE STANDARD C62.33-1982 SUBSECTION 2.3 AND 2.4)**

TERMS AND DESCRIPTIONS	SYMBOL
<b>Clamping Voltage.</b> Peak voltage across the varistor measured under conditions of a specified peak $V_C$ pulse current and specified waveform. NOTE: Peak voltage and peak currents are not necessarily coincidental in time.	$V_C$
<b>Rated Peak Single Pulse Transient Currents (Varistor).</b> Maximum peak current which may be applied for a single 8/20 $\mu$ s impulse, with rated line voltage also applied, without causing device failure.	$I_{TM}$
<b>Lifetime Rated Pulse Currents (Varistor).</b> Derated values of $I_{TM}$ for impulse durations exceeding that of an 8/20 $\mu$ s waveshape, and for multiple pulses which may be applied over device rated lifetime.	-
<b>Rated RMS Voltage (Varistor).</b> Maximum continuous sinusoidal RMS voltage which may be applied.	$V_{M(AC)}$
<b>Rated DC Voltage (Varistor).</b> Maximum continuous DC voltage which may be applied.	$V_{M(DC)}$
<b>DC Standby Current (Varistor).</b> Varistor current measured at rated voltage, $V_{M(DC)}$ .	$I_D$
For certain applications, some of the following terms may be useful.	
<b>Nominal Varistor Voltage.</b> Voltage across the varistor measured at a specified pulsed DC current, $I_{N(DC)}$ , of specific duration. $I_{N(DC)}$ is specified by the varistor manufacturer.	$V_{N(DC)}$
<b>Peak Nominal Varistor Voltage.</b> Voltage across the varistor measured at a specified peak AC current, $I_{N(AC)}$ , of specific duration. $I_{N(AC)}$ is specified by the varistor manufacturer.	$V_{N(AC)}$
<b>Rated Recurrent Peak Voltage (Varistor).</b> Maximum recurrent peak voltage which may be applied for a specified duty cycle and waveform.	$V_{PM}$
<b>Rated Single Pulse Transient Energy (Varistor).</b> Energy which may be dissipated for a single impulse of maximum rated current at a specified waveshape, with rated RMS voltage or rated DC voltage also applied, without causing device failure.	$W_{TM}$
<b>Rated Transient Average Power Dissipation (Varistor).</b> Maximum average power which may be dissipated due to a group of pulses occurring within a specified isolated time period, without causing device failure.	$P_{T(AV)M}$
<b>Varistor Voltage.</b> Voltage across the varistor measured at a given current, $I_X$ .	$V_X$
<b>Voltage Clamping Ratio (Varistor).</b> A figure of merit measure of the varistor clamping effectiveness as defined by the symbols $V_C/V_{M(AC)}$ , $V_C/V_{M(DC)}$ .	$\frac{V_C}{V_{PM}}$
<b>Nonlinear Exponent.</b> A measure of varistor nonlinearity between two given operating currents, $I_1$ and $I_2$ , as described by $I = kV^\alpha$ where k is a device constant, $I_1 \leq I \leq I_2$ , and $\alpha_{12} = \frac{\log I_2 / I_1}{\log V_2 / V_1}$	$\alpha$
<b>Dynamic Impedance (Varistor).</b> A measure of small signal impedance at a given operating point as defined by: $Z_X = \frac{dV_X}{dI_X}$	$Z_X$
<b>Resistance (Varistor).</b> Static resistance of the varistor at a given operating point as defined by: $R_X = \frac{V_X}{I_X}$	$R_X$
<b>Capacitance (Varistor).</b> Capacitance between the two terminals of the varistor measured at C specified frequency and bias.	C
<b>AC Standby Power (Varistor).</b> Varistor AC power dissipation measured at rated RMS voltage $V_{M(AC)}$ .	$P_D$
<b>Voltage Overshoot (Varistor).</b> The excess voltage above the clamping voltage of the device for a given current that occurs when current waves of less than 8 $\mu$ s virtual front duration are applied. This value may be expressed as a % of the clamping voltage ( $V_C$ ) for an 8/20 current wave.	$V_{OS}$
<b>Response Time (Varistor).</b> The time between the point at which the wave exceeds the clamping voltage level ( $V_C$ ) and the peak of the voltage overshoot. For the purpose of this definition, clamping voltage as defined with an 8/20 $\mu$ s current waveform of the same peak current amplitude as the waveform used for this response time.	-
<b>Overshoot Duration (Varistor).</b> The time between the point voltage level ( $V_C$ ) and the point at which the voltage overshoot has decayed to 50% of its peak. For the purpose of this definition, clamping voltage is defined with an 8/20 $\mu$ s current waveform of the same peak current amplitude as the waveform used for this overshoot duration.	-

# Application Note 9767

## How to Connect a Littelfuse Varistor

Transient suppressors can be exposed to high currents for short durations in the nanoseconds to millisecond time frame.

Littelfuse Varistors are connected in parallel to the load, and any voltage drop in the leads to the varistor will reduce its effectiveness. Best results are obtained by using short leads that are close together to reduce induced voltages and a low ohmic resistance to reduce  $I \cdot R$  drops.

## Electrical Connections

### Single Phase

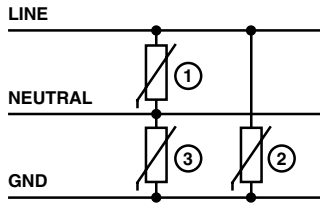
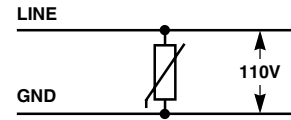
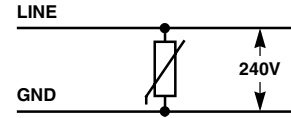


FIGURE 22.

SINGLE PHASE  
2 WIRE 110V



SINGLE PHASE  
2 WIRE 240V



SINGLE PHASE  
3 WIRE 120V/240V

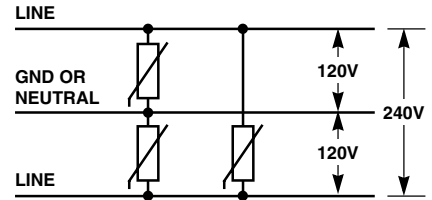


FIGURE 23.

### 3 Phase

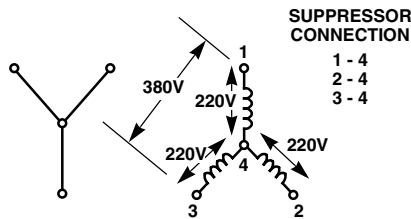


FIGURE 24A. 3 PHASE 220V/380V, UNGROUNDED

SUPPRESSOR CONNECTION  
1 - 4  
2 - 4  
3 - 4

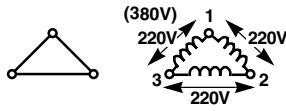


FIGURE 24B. 3 PHASE 220V OR 380V, UNGROUNDED

SUPPRESSOR CONNECTION  
1 - 2  
2 - 3  
3 - 1

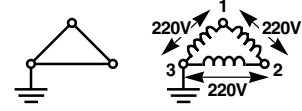


FIGURE 24C. 3 PHASE 220V, ONE PHASE GND

SUPPRESSOR CONNECTION  
1 - 2  
2 - 3  
1 - 3

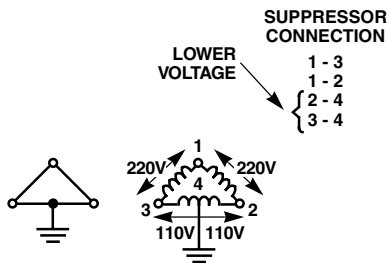
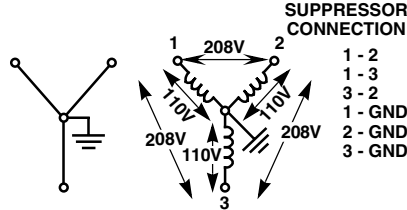


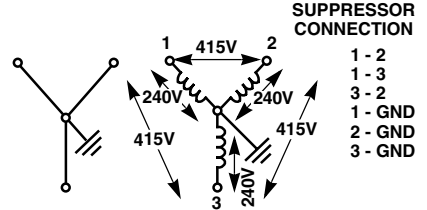
FIGURE 24D. 3 PHASE 220V

LOWER VOLTAGE  
SUPPRESSOR CONNECTION  
1 - 3  
1 - 2  
2 - 4  
3 - 4



If only 3 suppressor use 1-GND, 2-GND, 3-GND  
FIGURE 24E. 3 PHASE 120V/208V, 4-WIRE

SUPPRESSOR CONNECTION  
1 - 2  
1 - 3  
3 - 2  
1 - GND  
2 - GND  
3 - GND



If only 3 suppressor use 1-GND, 2-GND, 3-GND  
FIGURE 24F. 3 PHASE 240V/415V

SUPPRESSOR CONNECTION  
1 - 2  
1 - 3  
3 - 2  
1 - GND  
2 - GND  
3 - GND

For higher voltages use same connections, but select varistors for the appropriate voltage rating.

**DC Applications**

DC applications require connection between plus and minus or plus and ground and minus and ground.

For example, if a transient towards ground exists on all 3 phases (common mode transients) only transient suppressors connected phase to ground would absorb energy. Transient suppressors connected phase to phase would not be effective.

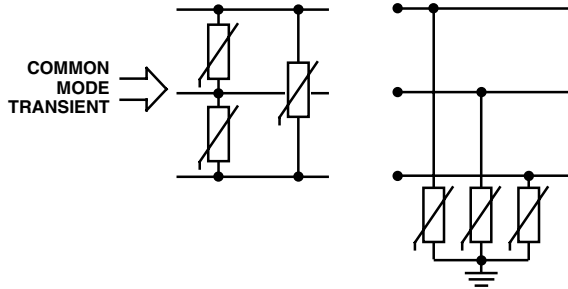


FIGURE 25A. INCORRECT      FIGURE 25B. CORRECT

FIGURE 25. COMMON MODE TRANSIENT AND CORRECT SOLUTION

On the other hand if a differential mode of transient (phase to phase) exists then transient suppressors connected phase to phase would be the correct solution.

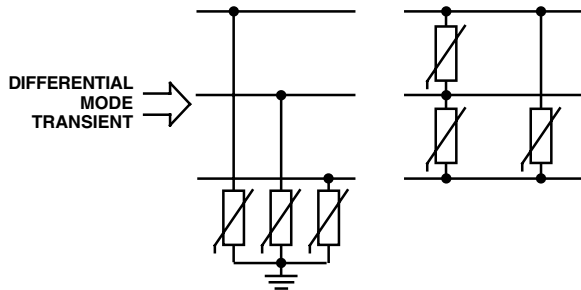


FIGURE 26A. INCORRECT      FIGURE 26B. CORRECT

FIGURE 26. DIFFERENTIAL MODE TRANSIENT AND CORRECT SOLUTION

This is just a selection of some of the more important variations in connecting transient suppressors.

The logical approach is to connect the transient suppressor between the points of the potential difference created by the transient. The suppressor will then equalize or reduce these potentials to lower and harmless levels.

**References**

For Littelfuse documents available on the web, see <http://www.littelfuse.com/>

- [1] Harnden, J.D., F.D. Martzloff, W.G. Morris and F.B. Golden, "The GEMOV® Varistor - The Super Alpha Varistor" Electronics, Vol. 45, No. 21, 1972, p. 91.
- [2] Morris, W.G., "Electrical Properties of ZnO-Bi<sub>2</sub>O<sub>3</sub> Ceramics," Journal of the Am. Ceram. Soc., Vol. 56, 1973.
- [3] Matsuoka, M., "Non-Ohmic Properties of Zinc Oxide Ceramics," Japanese Jnl. Appl. Phys., Vol. 10, 1971, p. 736.
- [4] Mahan, G., L. Levinson and H. Philipp, "Single Grain Junction Studies at ZnO Varistors Theory & Experiment," Report #78CRF160, General Electric, Schenectady, N.Y., 1978. Forthcoming in Applied Physics Letters.
- [5] Mahan, G., L. Levinson and H. Philipp, "Theory of Conduction in ZnO Varistors," Journal of Applied Physics (in press).
- [6] Levine, J.D., "Theory of Varistor Electronic Properties," Critical Review of Solid State Science, 5, 1975, pp. 597-608.
- [7] May, J.E., "Carrier Concentration and Depletion Layer Model of Zinc Oxide Varistors," Bulletin of the American Ceramic Society, Vol. 57, No. 3, 1978, p. 335.
- [8] Sze, S.M., "Physics of Semiconductor Devices," John Wiley & Sons, New York, N.Y., 1969.
- [9] Einzinger, R., "Microcontact Measurement of ZnO Varistors," Ber. Dt. Keram, Vol. 52, 1975, pp. 244-245.
- [10] Lou, L.F., "Current-Voltage Characteristics of ZnO-Bi<sub>2</sub>O<sub>3</sub> Heterojunction," Journal of Applied Physics, Vol. 50, 1979, p. 555.
- [11] Lou, L.F. "Semiconducting Properties of ZnO-Grain Boundary-ZnO Junctions in Ceramic Varistors," Appl. Phys. Letters, Vol. 36, 1980, pp. 570-572.
- [12] Lou, L.F., and J.E. May, Unpublished Research, General Electric, Syracuse, N.Y., 1981.
- [13] Morris, W., "Physical Properties of the Electrical Barriers in Varistors," J. Vac. Sci. Technol., 13, 1976, pp. 926-931.
- [14] Bernasconi, J., S. Strassler, B. Knecht, H. Klein and A. Menth, Solid State Communication, Vol. 21, 1977, pp. 867-869.
- [15] Pike, G. and C. Seager, "The DC Voltage Dependence of Semiconductor Grain-Boundary Resistance," Journal of Appl. Phys., Vol. 50, 1979, pp. 3414-3422